

Roles of energy eigenstates and eigenvalues in equilibration of isolated quantum systems

Shaoqi Zhu (朱少奇)¹ and Biao Wu (吴飙)^{1,2,3}

¹*International Center for Quantum Materials, School of Physics, Peking University, Beijing 100871, China*

²*Collaborative Innovation Center of Quantum Matter, Beijing 100871, China*

³*Wilczek Quantum Center, Department of Physics and Astronomy, Shanghai Jiao Tong University, Shanghai 200240, China*

(Received 24 April 2017; revised manuscript received 4 July 2017; published 12 October 2017)

We show that eigenenergies and energy eigenstates play different roles in the equilibration process of an isolated quantum system. Their roles are revealed numerically by exchanging the eigenenergies between an integrable model and a nonintegrable model. We find that the structure of eigenenergies of a nonintegrable model characterized by nondegeneracy ensures that quantum revival occurs rarely whereas the energy eigenstates of a nonintegrable model suppress the fluctuations for the equilibrated quantum state. Our study is aided with a quantum entropy that describes how randomly a wave function is distributed in quantum phase space. We also demonstrate with this quantum entropy the validity of Berry's conjecture for energy eigenstates. This implies that the energy eigenstates of a nonintegrable model appear indeed random.

DOI: [10.1103/PhysRevE.96.042124](https://doi.org/10.1103/PhysRevE.96.042124)

I. INTRODUCTION

How equilibration is achieved in an isolated quantum system is a fundamental issue regarding the foundation of quantum statistical mechanics. This issue has intrigued many physicists [1–3]. In standard textbooks on quantum statistical physics, one just assumes that quantum equilibration can be achieved and assigns the equilibrated state certain properties with postulates, such as equal *a priori* probability, to establish microcanonical ensemble. In his well-known textbook [4], Huang states, “The postulates of quantum statistical mechanics are to be regarded as working hypotheses whose justification lies in the fact that they lead to results in agreement with experiments. Such a point of view is not entirely satisfactory, because these postulates cannot be independent of, and should be derivable from, the quantum mechanics of molecular systems.” This issue has recently received renewed interest [5–21] due to experimental developments especially in ultracold atomic and molecular gases with remarkably high degree of isolation and high-precision control of parameters [22–24].

In 1929 von Neumann addressed this fundamental issue by proving quantum ergodic theorem and quantum H theorem [1,3], where he claimed, “in quantum mechanics one can prove the ergodic theorem and the H-theorem in full rigor and without disorder assumptions; thus, the applicability of the statistical-mechanical methods to thermodynamics is guaranteed without relying on any further hypotheses.” Now these two theorems have been reformulated in a more rigorous framework without invoking ambiguous coarse graining [7,14,20]; in particular, the quantum ergodic theorem is found to be closely related to a modern term, normal typicality [5,25]. It is clear in these studies that the structure of the quantum system's eigenenergies plays a crucial role: when the eigenenergies and their gaps are nondegenerate, then the two theorems hold and the isolated quantum system can equilibrate. The form of energy eigenstates, that is, how they distribute either in position space or in momentum space, is not important in these studies. This is, of course, in agreement with the Gibbs distribution at equilibrium, which is solely determined by the energies and density of states. Due to its fundamental role in quantum equilibration, the structure of eigenenergies was used to give a precise definition of quantum ergodicity and quantum mixing [21].

Recently, a different point of view on quantum equilibration, which was already mentioned in Landau's book as a footnote [26], has received a great deal of attention. This view is eigenstate thermalization hypothesis (ETH), which is justified on the basis of random matrix theory [27] and Berry's conjecture [28–30]. According to ETH, the form of energy eigenstates is crucial. In integrable systems, the eigenstates look rather regular and are not thermalized; in nonintegrable systems, the eigenstates should look random according to Berry's conjecture and are therefore thermalized. Many numerical and theoretical results [30–39] on real many-body systems including integrable and nonintegrable systems turn out to support this hypothesis and this has stimulated enormous research on many-body localization [40–46].

Although these two points of view are different, they do not contradict each other. Most importantly, they agree on one very important point: only nonintegrable isolated quantum systems can equilibrate or thermalize. In this paper we try to clarify the roles played by eigenenergies and energy eigenstates in quantum equilibration by comparing an integrable model and a nonintegrable model and exchanging their eigenenergies.

For an isolated quantum system, its dynamics is given by

$$|\psi(t)\rangle = \sum_n a_n e^{-iE_n t/\hbar} |\phi_n\rangle, \quad (1)$$

where $|\phi_n\rangle$ is an energy eigenstate with eigenenergy E_n . The coefficients a_n are independent of time and determined by the initial state. The dynamics is clearly controlled by both eigenstates $|\phi_n\rangle$ and eigenenergies E_n . For a given quantum system, if it is integrable, then both $|\phi_n\rangle$ and E_n show characteristics of an integrable system; if it is nonintegrable, then both $|\phi_n\rangle$ and E_n are embedded with the features of a nonintegrable system. However, numerically, we can have a dynamics that is controlled by a set of integrable eigenenergies E_n with a set of nonintegrable eigenstates $|\phi_n\rangle$. Consider two models, one is integrable and the other is nonintegrable. Suppose their eigenstates and eigenenergies are, respectively, $\{|\phi_n^i\rangle, E_n^i\}$ and $\{|\phi_n^c\rangle, E_n^c\}$. By exchanging the two sets of eigenenergies, we can numerically have four different dynamical evolutions: (i) integrable eigenstates and integrable eigenenergies, (ii)

integrable eigenstates and nonintegrable eigenenergies, (iii) nonintegrable eigenstates and integrable eigenenergies, (iv) nonintegrable eigenstates and nonintegrable eigenenergies. For example, the third dynamics can be expressed as

$$|\psi'(t)\rangle = \sum_n a_n e^{-iE_n^i t/\hbar} |\phi_n^c\rangle. \quad (2)$$

The second and third dynamics never occurs in a real physical system. However, by studying them we are able to clarify the roles played by energy eigenstates and eigenenergies in dynamics: the nondegeneracy of eigenenergies ensures that the initial state is dephased over time and quantum revival is suppressed; the randomness in the nonintegrable eigenstates keeps the fluctuations around the equilibrium small. Therefore, nondegenerate eigenenergies and randomized eigenstates are equally important for quantum equilibration of a nonintegrable system but playing different roles.

In our numerical study, we use the quantum entropy for pure states introduced in Ref. [20] to quantify the equilibration process. This quantum entropy is defined by projecting a wave function unitarily to phase space and describes how a wave function is distributed in phase space. The more randomly the wave function is distributed the bigger the entropy. In the second part of our paper, we use this entropy to check the validity of Berry's conjecture [47] and show that the eigenfunctions of a nonintegrable system indeed look random. Our study finds that the quantum entropy for energy eigenstates agrees very well with Berry's conjecture at each energy level and the entropy fluctuation among different eigenstates is very small for the fully chaotic systems. Note that the validity of Berry's conjecture has been checked previously with autocorrelation functions [48], amplitude distributions [49–51], and statistics of nodal domains [52].

We organize the paper as follows. In Sec. II, we briefly describe ripple billiards, and quantum phase space, and the concept of quantum entropy for pure states. In Sec. III, we compare the time evolution of a Gaussian wave packet moving in a square billiard and a ripple billiard, representing integrable and nonintegrable systems, respectively. We then exchange their eigenenergies to create two artificial dynamics. By comparing these different dynamics, we are able to identify the roles of eigenenergies and eigenfunctions in quantum equilibration of an isolated system. Section IV is to explain why eigenfunctions in a chaotic system can play the role identified in the preceding section. This is achieved by comparing them to the wave functions constructed according to Berry's conjecture. We conclude in Sec. V.

II. MODEL AND QUANTUM ENTROPY FOR PURE STATE

In this section, we briefly introduce the models for our numerical calculation, quantum phase space, and the quantum entropy for pure states that we use to characterize the quantum equilibration.

In our numerical calculation, we use the model of ripple billiard [53], which is shown in Fig. 1. When $a = 0$, it becomes the square billiard and it is an integrable system. When $a > 0$, it is nonintegrable. In general, as a becomes larger, the billiard is more chaotic [53]. The billiard is special in that the elements of its Hamiltonian can be calculated analytically. As a result,

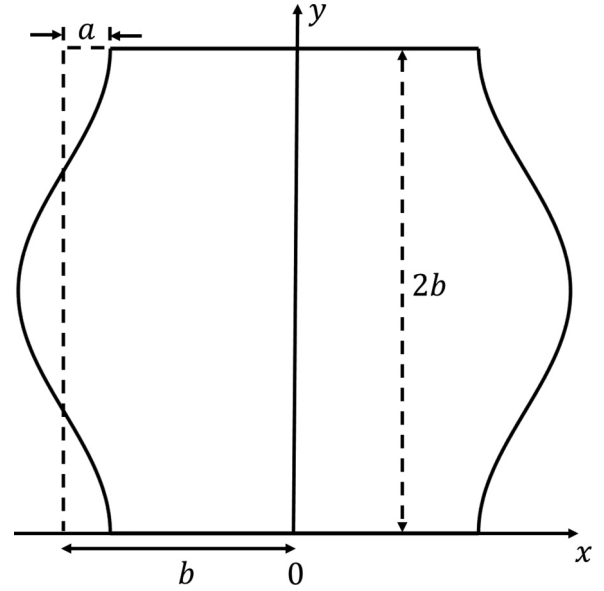


FIG. 1. Ripple billiard. The two curved boundaries are given by $x = \pm b \mp a \cos(\pi y/b)$, respectively.

one can conveniently study its eigenenergies and eigenstates in a systematic way. Details can be found in Ref. [53]. It would be interesting to examine other models [54] in the future; in this paper, we focus on our simple model.

The nearest-neighbor level spacing statistics follows a Poisson distribution for the integrable system with many energy degeneracies, while it follows a Wigner-Dyson distribution for the nonintegrable system with no energy degeneracy in the even-even modes. The distributions are shown in Fig. 2.

Besides the well-known von Neumann entropy, another quantum entropy was introduced by von Neumann in his 1929 paper [1]. This quantum entropy was defined for pure states. However, von Neumann's definition involves ambiguous coarse graining, making numerical computation impossible. In Ref. [20], von Neumann's definition was modified and a new quantum entropy for pure states was defined with Wannier functions obtained with Kohn's method [55]. To define this entropy, we need first to construct a quantum phase space: (i) the classical phase space is divided into Planck cells; (ii) each Planck cell is assigned a Wannier function and all the Wannier functions form a set of a complete orthonormal basis [20]. The Wannier functions are constructed by orthonormalizing a set of Gaussian wave packets of width ζ ,

$$g_{j_x, j_k} \equiv \exp \left[-\frac{(x - j_x x_0)^2}{4\zeta^2} + i j_k k_0 x \right], \quad (3)$$

where j_x and j_k are integers. When $x_0 k_0 = 2\pi$, this set of the resulted Wannier functions is complete. In this paper, parameters are chosen as $x_0 = 1, k_0 = 2\pi$, and $\zeta = (2\pi)^{-1}$. The details of this construction of quantum phase space can be found in Ref. [20]. Once the Wannier functions are obtained, they are used to project a wave function unitarily onto the quantum phase space. To give unfamiliar readers a sense of this quantum phase space, the 100th eigenfunction of a one-dimensional harmonic oscillator is mapped in this

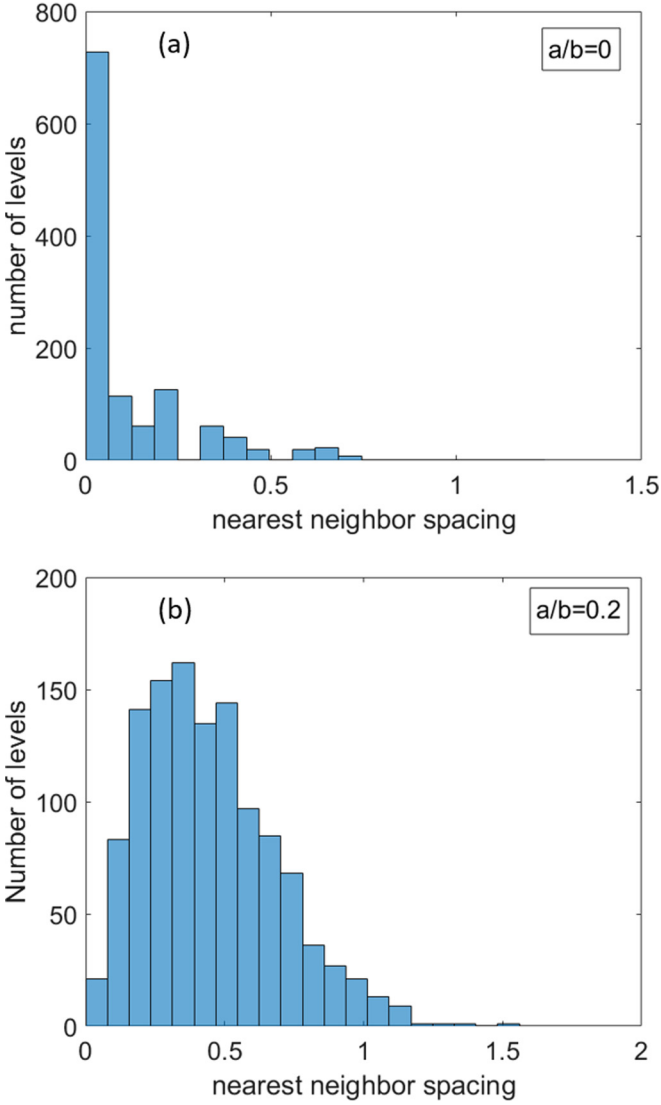


FIG. 2. Nearest-neighbor level spacing statistics for square billiard $a/b = 0$ in (a) and ripple billiard $a/b = 0.2$ in (b) with even-even modes.

quantum phase space and is shown in Fig. 3. The wave function concentrates on the classical trajectory.

If $|w_j\rangle$ is the Wannier function at Planck cell j , then $|\langle\psi|w_j\rangle|^2$ is the probability at Planck cell j for a wave function ψ . Our quantum entropy for pure state ψ is defined with these probabilities as

$$S_w(\psi) \equiv - \sum_j \langle\psi|W_j|\psi\rangle \ln \langle\psi|W_j|\psi\rangle, \quad (4)$$

where $W_j \equiv |w_j\rangle\langle w_j|$ is the projection to Planck cell j . It is clear from this definition that the entropy $S_w(\psi)$ describes how a quantum state ψ is spread out in the phase space: the more Planck cells that ψ occupies the bigger its entropy.

In our numerical calculation, length is in an arbitrary unit of L . Correspondingly, the wave vector k is in unit of $1/L$ and the energy is in unit of $\hbar^2/2mL^2$, where m is the particle mass. Throughout this paper we omit these units for convenience. For example, when we say $b = 5.5$ we mean $b = 5.5L$. The

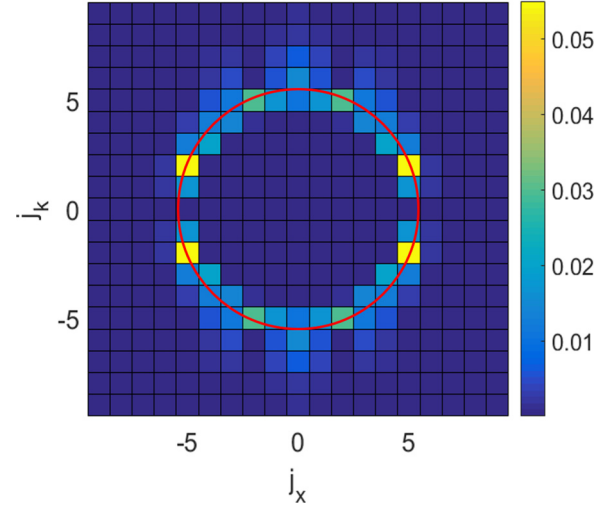


FIG. 3. The 100th eigenfunction of a one-dimensional harmonic oscillator in the quantum phase space. The red circle is the corresponding classical trajectory. j_x and j_k are indices labeling Planck cells.

j in w_j stands for $\{j_x, j_k\}$ in a one-dimensional system and $\{j_x, j_y, j_k, j_l\}$ in a two-dimensional system.

Here are the details on the quantum phase space in our numerical calculation. Taking $b = 5.5$, $a/b = 0.2$ for example, the ripple billiard is confined in a rectangle area 13.2×11 . Every Planck cell in position space is 1×1 . When we map a wave function in a ripple billiard onto the phase space, we need $N_{j_x} = 13 \times 11$ position indices with $j_x \in [-6, 6]_{\mathbb{Z}}$ and $j_y \in [1, 11]_{\mathbb{Z}}$ to cover the whole real space. The maximum wavelength corresponding to the energy scale in our numerical computation is $|k| = 4 \times 2\pi$. Therefore, we need $N_{j_k} = 9 \times 9$ momentum indices with $j_k = [-4, 4]_{\mathbb{Z}}$ in both the k_x direction and the k_y direction. The total number of Planck cells is $N = N_{j_x} \times N_{j_k}$. If the wave function ψ distributes equally in the N Planck cells, the entropy would be $S_{\max} = \ln N$. The mesh points is 180×180 dividing the billiard into numerically discrete area.

III. TIME EVOLUTION

Our main aim of this paper is to identify the roles played by eigenstates and eigenenergies in quantum dynamics, particularly in the dynamics that leads to equilibration. For this purpose, we choose two different billiards: (i) square billiard ($a/b = 0$); (ii) chaotic ripple billiard ($a/b = 0.2$). We not only study and compare their dynamics but also create two artificial dynamics by exchanging these two billiards' eigenenergies. Let $\{|\phi_n^i\rangle, E_n^i\}$ be the set of eigenstates and eigenenergies for the square billiard and $\{|\phi_n^c\rangle, E_n^c\}$ be the set of eigenstates and eigenenergies for the ripple billiard. The dynamics of these two billiards can be described formally as

$$|\psi_i(t)\rangle = \sum_n a_n e^{-iE_n^i t/\hbar} |\phi_n^i\rangle, \quad (5)$$

and

$$|\psi_c(t)\rangle = \sum_n b_n e^{-iE_n^c t/\hbar} |\phi_n^c\rangle, \quad (6)$$

where the coefficients a_n 's and b_n 's are determined by the initial condition. By exchanging their eigenenergies, we can create two more dynamics

$$|\psi_{ic}(t)\rangle = \sum_n a_n e^{-iE_n^c t/\hbar} |\phi_n^i\rangle, \quad (7)$$

and

$$|\psi_{ci}(t)\rangle = \sum_n b_n e^{-iE_n^i t/\hbar} |\phi_n^c\rangle. \quad (8)$$

These two dynamics are artificial but will help us to identify the roles of eigenstates and eigenenergies.

The numerical results of these four dynamics are shown in Fig. 4. The initial state for these four different dynamics is the same and it is a moving Gaussian wave packet,

$$\Psi(0) = \exp\left[-\frac{x^2 + (y-b)^2}{4\sigma^2} + i(k_x x + k_y y)\right]. \quad (9)$$

With numerically computed eigenfunctions $|\phi_n^i\rangle$ and $|\phi_n^c\rangle$, we determine the coefficients a_n 's and b_n 's. This allows us to find the wave functions at any time t . We finally compute the entropies for these wave functions with Eq. (4). How the entropies change with time is shown in Fig. 4.

There are four very different dynamics in Fig. 4. In case (a) (integrable eigenstates and integrable eigenenergies), the entropy oscillates regularly with time with large amplitudes. In case (b) (integrable eigenstates and nonintegrable eigenenergies), the entropy increases quickly to a large value and stays at this value with relatively large fluctuations. In case (c) (nonintegrable eigenstates and integrable eigenenergies), the entropy similarly relaxes quickly to a large value with small fluctuations. However, the entropy drops back almost to its initial value after a certain period. This period is consistent with the oscillation period in the case (a). This is the well-known phenomenon of quantum revival. The period of quantum revival is determined by energy differences $E_m - E_n$ in the off-diagonal terms in the evolution.

$$|\psi(t)\rangle\langle\psi(t)| = \sum_n |a_n|^2 |\phi_n\rangle\langle\phi_n| + \sum_{m \neq n} a_m^* a_n e^{i(E_m - E_n)t/\hbar} |\phi_m\rangle\langle\phi_n|. \quad (10)$$

The eigenenergies of the integrable square billiard system have an expression as $E_{gh} = (\pi/2b)^2(m_1^2 + m_2^2)$, where m_1 and m_2 are positive integers. So the smallest nonzero energy difference is $\Delta E_s = (\pi/2b)^2$. Other energy differences are integral multiples of ΔE_s . Therefore, the period of quantum revival is the period corresponding to the smallest energy difference $2\pi\hbar/\Delta E_s$, which agrees with the period seen in Figs. 4(a), 4(c). In case (d) (nonintegrable eigenstates and nonintegrable eigenenergies), the entropy quickly relaxes to its maximum value and stays there with very small fluctuations. There is no quantum revival.

The results in Fig. 4 are quite revealing. To reach quantum equilibrium as in Fig. 4(d), we need both nonintegrable eigenstates and nonintegrable eigenenergies. The nonintegrable eigenstates ensure that the fluctuations are small once

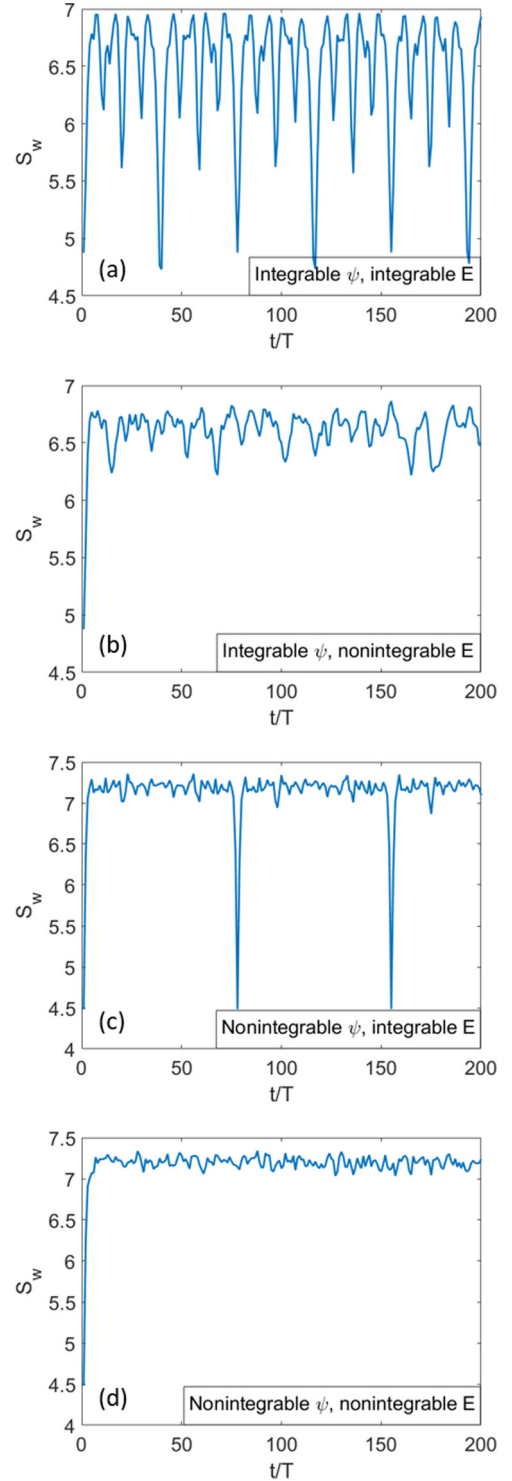


FIG. 4. Time evolution for the quantum entropy in four situations: (a) integrable eigenstates and integrable eigenenergies; (b) integrable eigenstates and nonintegrable eigenenergies; (c) nonintegrable eigenstates and integrable eigenenergies; (d) nonintegrable eigenstates and nonintegrable eigenenergies. The scale of the ripple billiard is $a = 1.1, b = 5.5$ while the length of side for the square billiard is b . Initial Gaussian wave packet parameters: $\sigma = 1, k_y = 0; k_x = a + b$ for ripple billiard and $k_x = b$ for square billiard. T is the time when the envelope of the initial wave packet with group velocity $V_g = 2k_x$ return to the center of the billiard after reflecting once from one boundary along x direction. L is the length unit; $1/L$ is the unit for k .

the equilibrium is reached. The nonintegrable eigenenergies guarantee no occurrence of large deviation in a physically meaningful time. These two important points are not hard to understand intuitively: the nonintegrable eigenenergies lack of degeneracy in eigenenergies and their gaps that is needed for regular quantum dynamics; the nonintegrable eigenstates are rather random according to Berry's conjecture. The former has been discussed extensively in Refs. [1,7,20,21]. We will examine the latter in detail in the next section.

Before we proceed further, we offer a few remarks on quantum revival to avoid potential misunderstanding. (i) The quantum revival in the square billiard does not depend on its initial condition. (ii) Quantum revival occurs in integrable systems [56]; however, integrability does not mean that there is quantum revival for all observables [57,58]. The latter does not contradict our statement that the structure of eigenenergies of nonintegrable systems ensures that there is no frequent quantum revival.

IV. ENTROPY FOR EIGENSTATES AND BERRY'S CONJECTURE

In the preceding section, we see that nonintegrable eigenstates are essential to keep the fluctuations small at equilibrium. The intuitive reason is that these nonintegrable eigenstates are random according to Berry's conjecture, which is the base for ETH [28]. However, there are two important issues that have so far no satisfactory answers. The first one is how to measure quantitatively the randomness in eigenstates. If there is such a measure of randomness, how does the eigenwave-function constructed artificially according to Berry's conjecture compare to the real eigenstates? The other issue is that there are many quantum scar eigenstates. These eigenstates look regular as their amplitudes concentrate along classical periodical orbits [59]. How often do they appear? If there is a quantitative measure of randomness, how far do these quantum scar states deviate from other eigenstates? We examine these two issues in this section.

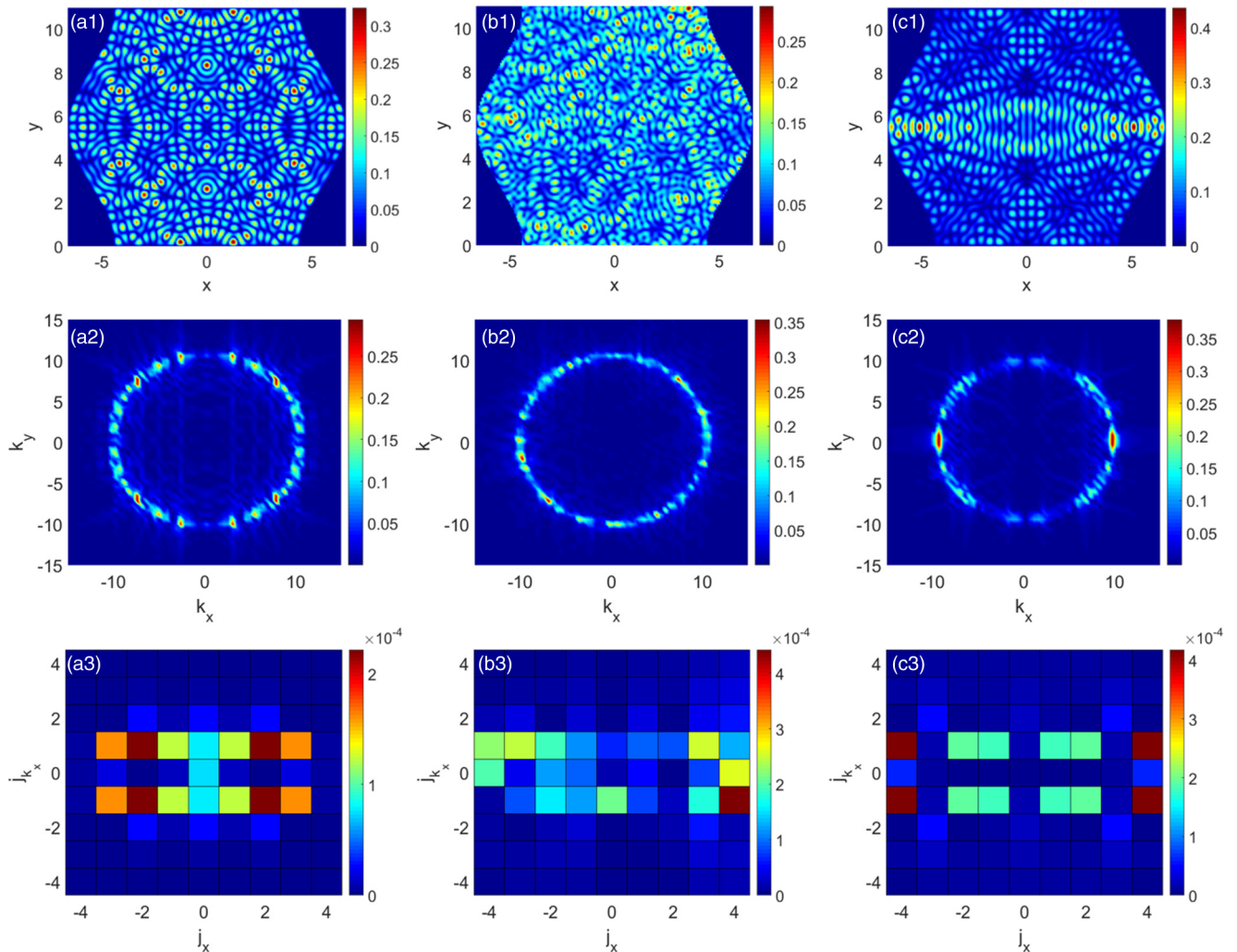


FIG. 5. (a1) the 1000th eigenstate in the position space; (b1) the corresponding wave function ψ_B constructed according to Berry's conjecture in the position space; (c1) the 857th eigenstate (which is a scar state) in the position space. (a2), (b2), (c2) Their respective representation in the momentum space. (a3), (b3), (c3) Their representations in the quantum phase space with the position and momentum along the y direction fixed at $j_y = 5, j_{k_y} = 0$. For the billiard, $a = 0.55$ and $b = 5.5$. L is the unit of length.

The quantum entropy $S_w(\psi)$ defined in Eq. (4) is a good measure of the randomness in eigen-wave-functions. As the wave function is projected unitarily onto the quantum phase space, $S_w(\psi)$ contains information both in position and momentum. In contrast, the probability $\psi(x)$ [$\psi(k)$] has information only in position (or momentum). We shall use it to measure the randomness in eigen-wave-functions.

Berry's conjecture states that each eigenfunction of a classically chaotic quantum billiard system is a superposition of plane waves with random phase and Gaussian random amplitude but with the same wavelength [28,47]. Mathematically, such a wave function with wavelength k can be expressed as

$$\psi_B = \int dk A(\mathbf{k}) \exp\{-i[\mathbf{k} \cdot \mathbf{r} + \theta(\mathbf{k})]\}, \quad (11)$$

where the modulus of \mathbf{k} is fixed but it can point to any direction. Amplitude $A(\mathbf{k})$ is a Gaussian random distribution for k in different direction. $\theta(\mathbf{k})$ is the random phase.

For comparison, we calculate the wave functions ψ_B for every wavelength k that corresponds to an eigenstate of the ripple billiards. We first look at an example, where ψ_B is computed with the wavelength corresponding to the 1000th eigenstate for the ripple billiard ($a = 0.55, b = 5.5$). These two wave functions are plotted in Fig. 5 with the 857th eigenstate, which is a scar state [59]. The wave functions are compared in three different spaces: in position space, in momentum space, and in quantum phase space. It is clear from the figure that the 1000th eigenstate and its corresponding ψ_B are qualitatively similar: both their wave functions are quite spread out in all these three spaces. This is confirmed by our entropy: for the 1000th eigenstate $S_w = 7.11$; for the Berry wave function ψ_B , $S_w = 7.09$. As a scar state, the 857th eigenstate looks qualitatively different from the 1000th eigenstate. In the position space, the 857th eigenstate concentrates on a

periodic trajectory that describes a classical particle bouncing horizontally in the middle of the billiard. As a result, its momentum distribution concentrates along certain directions and its distribution in the phase space focuses on some areas. Quantitatively, its entropy is $S_w = 6.57$, significantly smaller than the other two wave functions. Note that ψ_B is constructed without respecting the symmetry of the system so that it does not have the symmetries that we see in the 1000th and 857th eigenstate.

We now compare the Berry wave functions ψ_B and the eigenstates of ripple billiards systematically. For a given billiard, the entropies are computed for its eigenstates from the first to 1200th and their corresponding Berry wave functions ψ_B . The results for five different billiards are shown in Fig. 6, where the blue lines are for the eigenstates and the red lines are for ψ_B . For the billiard with $a/b = 0.01$, we see that the entropies of eigenstates have a general trend to increase with energy levels and this trend is shared by the Berry wave functions ψ_B . However, the entropies of eigenstates have much larger fluctuations compared to ψ_B . As we increase the ratio a/b and the billiard gets more chaotic [19,53], the general trend of the entropy does not change. However, the fluctuations become smaller. This is quantitatively shown in the last panel. Our numerical observation is that the large fluctuations for the billiards with $a/b \geq 0.1$ are caused by scar states, which is about 10% of all the eigenstates. Note that for the billiards with small a/b , they are near integrable and it is hard to distinguish scar states and other regular-looking eigenstates.

We have also averaged the entropy over every nearest 30 eigenstates. The results are plotted as yellow lines in Fig. 6. Even for near-integrable billiards, the averaged entropy agrees well with the entropy of the Berry wave function ψ_B with small fluctuations. The agreement improves as the ratio a/b

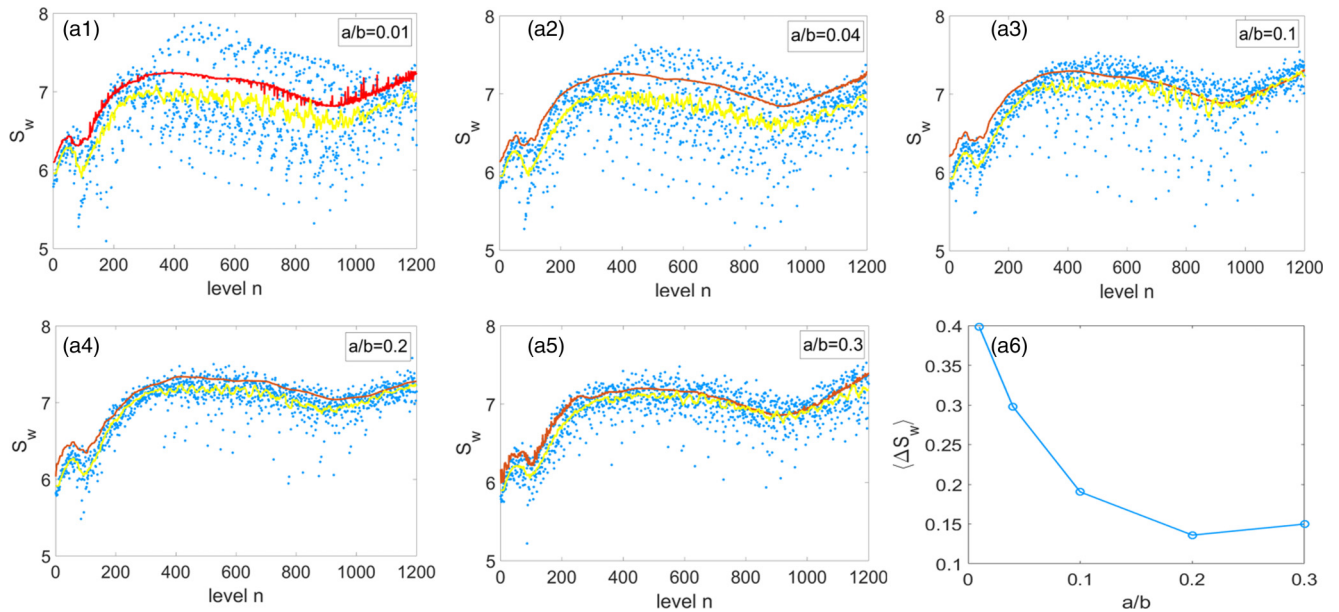


FIG. 6. (a1)–(a5) Quantum pure state entropy S_w of eigenfunctions of the ripple billiards and their corresponding ψ_B constructed according to Berry's conjecture. The x axis is the eigenenergy level. Blue lines represent the results of the ripple billiard; red lines represent the results for ψ_B . Yellow lines are obtained from the blue dots by averaging the nearest 30 eigenstates (the standard microcanonical ensemble average). (a6) Average entropy fluctuation around its microcanonical ensemble average for different a/b .

increases. Such an agreement implies that once the averaging is over a large number of eigenstates how each eigenstate looks is no longer important. This shows that the postulate of equal *a priori* probability in standard textbooks [4] over an energy shell of many eigenstates is valid even for integrable systems. That is why it is not necessary to discuss the integrability of a system in standard textbooks on quantum statistical mechanics [4,26]. This also implies that ETH is not a necessary condition for equilibration of a closed quantum systems. This agrees with the numerical results in Ref. [36].

Though the billiard model is a single-particle system, we believe our results are also applicable for interacting system for the following reasons. (i) The energy level spacing statistics is related to the integrability of a system, whether it has a single particle or interacting many particles. This is manifested by the fact that the energy level spacing statistics can be explained with the random matrix theory. In fact, the random matrix theory was developed to explain the energy levels of a nucleus, which consists of interacting protons and neutrons [60]. It was found later that this theory also works for single-particle chaotic systems [27]. (ii) In Ref. [28], Berry's conjecture was applied to interacting systems to establish ETH. Therefore, our results regarding eigenfunctions also apply for interacting systems wherever Berry's conjecture works.

V. CONCLUSIONS

We have identified the roles of eigenstates and eigenenergies in quantum equilibration of an isolated system. This is achieved by exchanging the set of eigenenergies between an integrable system and a chaotic system in our numerical simulations. Both the nondegeneracy of eigenenergies and the randomness in eigenstates are equally important for a nonintegrable system to achieve equilibration. The nondegeneracy of eigenenergies ensures the initial state is dephased over time and that the quantum revival is suppressed. The randomness in the nonintegrable eigenstates keeps the fluctuations around the equilibrium small. We have also shown in terms of a quantum pure state entropy that Berry's conjecture can quantitatively captures the randomness of the eigenstates.

ACKNOWLEDGMENTS

We thank X. Han for helpful discussions and D. Zhang for his codes on triangular billiard. This work was supported by the National Basic Research Program of China (Grant No. 2013CB921903) and the National Natural Science Foundation of China (Grants No. 11334001 and No. 11429402).

-
- [1] J. von Neumann, *Zeitschrift für Physik* **57**, 30 (1929).
 - [2] J. von Neumann, *Eur. Phys. J. H* **35**, 201 (2010).
 - [3] S. Goldstein, J. L. Lebowitz, R. Tumulka, and N. Zanghi, *Eur. Phys. J. H* **35**, 173 (2010).
 - [4] K. Huang, *Statistical Mechanics* (Wiley, New York, 1987).
 - [5] S. Goldstein, J. L. Lebowitz, R. Tumulka, and N. Zanghi, *Phys. Rev. Lett.* **96**, 050403 (2006).
 - [6] S. Popescu, A. J. Short, and A. Winter, *Nature Phys.* **2**, 754 (2006).
 - [7] P. Reimann, *Phys. Rev. Lett.* **101**, 190403 (2008).
 - [8] N. Linden, S. Popescu, A. J. Short, and A. Winter, *Phys. Rev. E* **79**, 061103 (2009).
 - [9] B. V. Fine, *Phys. Rev. E* **80**, 051130 (2009).
 - [10] T. N. Ikeda, Y. Watanabe, and M. Ueda, *Phys. Rev. E* **84**, 021130 (2011).
 - [11] V. I. Yukalov, *Laser Phys, Lett.* **8**, 485 (2011).
 - [12] C. Gogolin, M. P. Müller, and J. Eisert, *Phys. Rev. Lett.* **106**, 040401 (2011).
 - [13] A. Riera, C. Gogolin, and J. Eisert, *Phys. Rev. Lett.* **108**, 080402 (2012).
 - [14] A. J. Short, *New Journal of Physics* **13**, 053009 (2011).
 - [15] P. Reimann and M. Kastner, *New Journal of Physics* **14**, 043020 (2012).
 - [16] S. Sugiura and A. Shimizu, *Phys. Rev. Lett.* **108**, 240401 (2012).
 - [17] S. Sugiura and A. Shimizu, *Phys. Rev. Lett.* **111**, 010401 (2013).
 - [18] Q. Zhuang and B. Wu, *Laser Phys, Lett.* **11**, 085501 (2014).
 - [19] Q. Zhuang and B. Wu, *Phys. Rev. E* **88**, 062147 (2013).
 - [20] X. Han and B. Wu, *Phys. Rev. E* **91**, 062106 (2015).
 - [21] D. Zhang, H. T. Quan, and B. Wu, *Phys. Rev. E* **94**, 022150 (2016).
 - [22] D. A. Smith, M. Gring, T. Langen, M. Kuhnert, B. Rauer, R. Geiger, T. Kitagawa, I. Mazets, E. Demler, and J. Schmiedmayer, *New J. Phys.* **15**, 075011 (2013).
 - [23] L. Niu, P. Tang, B. Yang, X. Chen, B. Wu, and X. Zhou, *Phys. Rev. A* **94**, 063603 (2016).
 - [24] A. Polkovnikov, K. Sengupta, A. Silva, and M. Vengalattore, *Rev. Mod. Phys.* **83**, 863 (2011).
 - [25] S. Goldstein, J. L. Lebowitz, C. Mastrodonato, R. Tumulka, and N. Zanghi, *Proc. R. Soc. A* **466**, 3203 (2009).
 - [26] L. Landau and E. Lifshitz, *Statistical Mechanics* (Pergamon, Oxford, 1980), p. 360.
 - [27] H.-J. Stockmann, *Quantum Chaos: An Introduction* (Cambridge University Press, Cambridge, 1999).
 - [28] M. Srednicki, *Phys. Rev. E* **50**, 888 (1994).
 - [29] J. M. Deutsch, *Phys. Rev. A* **43**, 2046 (1991).
 - [30] M. Rigol, V. Dunjko, and M. Olshanii, *Nature (London)* **452**, 854 (2008).
 - [31] M. Rigol, V. Dunjko, V. Yurovsky, and M. Olshanii, *Phys. Rev. Lett.* **98**, 050405 (2007).
 - [32] M. Rigol and M. Srednicki, *Phys. Rev. Lett.* **108**, 110601 (2012).
 - [33] T. N. Ikeda, Y. Watanabe, and M. Ueda, *Phys. Rev. E* **87**, 012125 (2013).
 - [34] H. Kim, T. N. Ikeda, and D. A. Huse, *Phys. Rev. E* **90**, 052105 (2014).
 - [35] G. De Palma, A. Serafini, V. Giovannetti, and M. Cramer, *Phys. Rev. Lett.* **115**, 220401 (2015).
 - [36] A. Khodja, R. Steinigeweg, and J. Gemmer, *Phys. Rev. E* **91**, 012120 (2015).
 - [37] P. Hosur and X.-L. Qi, *Phys. Rev. E* **93**, 042138 (2016).
 - [38] F. Borgonovi, F. Izrailev, L. Santos, and V. Zelevinsky, *Phys. Rep.* **626**, 1 (2016).
 - [39] R. Steinigeweg, A. Khodja, H. Niemeyer, C. Gogolin, and J. Gemmer, *Phys. Rev. Lett.* **112**, 130403 (2014).
 - [40] A. Pal and D. A. Huse, *Phys. Rev. B* **82**, 174411 (2010).

- [41] R. Mondaini and M. Rigol, *Phys. Rev. A* **92**, 041601 (2015).
- [42] R. Nandkishore and D. A. Huse, *Annu. Rev. Condens. Matter Phys.* **6**, 15 (2015).
- [43] S. Bera, H. Schomerus, F. Heidrich-Meisner, and J. H. Bardarson, *Phys. Rev. Lett.* **115**, 046603 (2015).
- [44] X. Li, S. Ganeshan, J. H. Pixley, and S. Das Sarma, *Phys. Rev. Lett.* **115**, 186601 (2015).
- [45] R. Vosk, D. A. Huse, and E. Altman, *Phys. Rev. X* **5**, 031032 (2015).
- [46] M. Serbyn, Z. Papić, and D. A. Abanin, *Phys. Rev. X* **5**, 041047 (2015).
- [47] M. V. Berry, *J. Phys. A: Math. Gen.* **10**, 2083 (1977).
- [48] M. Shapiro and G. Goelman, *Phys. Rev. Lett.* **53**, 1714 (1984).
- [49] P. Sëba, *Phys. Rev. Lett.* **64**, 1855 (1990).
- [50] H. Alt, H. D. Gräf, H. L. Harney, R. Hofferbert, H. Lengeler, A. Richter, P. Schardt, and H. A. Weidenmüller, *Phys. Rev. Lett.* **74**, 62 (1995).
- [51] A. Kudrolli, V. Kidambi, and S. Sridhar, *Phys. Rev. Lett.* **75**, 822 (1995).
- [52] G. Blum, S. Gnutzmann, and U. Smilansky, *Phys. Rev. Lett.* **88**, 114101 (2002).
- [53] W. Li, L. E. Reichl, and B. Wu, *Phys. Rev. E* **65**, 056220 (2002).
- [54] G. A. Luna-Acosta, J. A. Méndez-Bermúdez, and F. M. Izrailev, *Phys. Rev. E* **64**, 036206 (2001).
- [55] W. Kohn, *Phys. Rev. B* **7**, 4388 (1973).
- [56] R. Robinett, *Physics Reports* **392**, 1 (2004).
- [57] L. F. Santos, F. Borgonovi, and F. M. Izrailev, *Phys. Rev. Lett.* **108**, 094102 (2012).
- [58] L. F. Santos, F. Borgonovi, and F. M. Izrailev, *Phys. Rev. E* **85**, 036209 (2012).
- [59] E. J. Heller, *Phys. Rev. Lett.* **53**, 1515 (1984).
- [60] O. Bohigas, R. Haq, and A. Pandey, in *Nuclear Data for Science and Technology* (Springer, Berlin, 1983), pp. 809–813.